Rho Meson Broadening in Hot and Dense Hadronic Matter

Song Gao[1], Charles Gale[2], Christoph Ernst[1],

Horst Stöcker[1] and Walter Greiner[1]

[1]*Institut für Theoretische Physik der J.W. Goethe-Universität*

Postfach 111932, D-60054 Frankfurt a. M., Germany

[2]*Physics Department, McGill University*

3600 University St., Montréal, QC, H3A 2T8, Canada

Abstract

The modification of the width of rho mesons due to in-medium decays and collisions is evaluated. The decay width is calculated from the imaginary part of the one-loop self-energy at finite temperature. The collision width is related to the cross sections of the ρ + pion and the ρ + nucleon reactions. A calculation based on an effective Lagrangian shows the importance of including the direct $\rho\pi \to \rho\pi$ scattering which is dominated by the a_1 exchange. A large broadening of the spectral function is found, accompanied by a strength suppression at the pole.

PACS : 25.75.Dw, 14.40Cs, 21.65.+f, 13.75.Lb

I. INTRODUCTION

It is generally believed that ultrarelativistic heavy ion collisions produce matter far from the ground state and provide conditions of high temperature and/or high density suitable for investigating modified particle properties in the medium. The vector mesons, e.g. the rho, are particularly important components of the matter produced in ultrarelativistic heavy ion collisions. It has been speculated that the restoration of chiral symmetry induces a mass shift of the ρ meson [1]. The direct dilepton decay channel, $\rho \to e^+e^-$, appears to be an ideal probe for studying the in-medium properties of the ρ: a possible mass shift, a modified dispersion relation, or a width modification [2–8]. Unfortunately, due to the interplay between those effects, it seems to be difficult to isolate the different effects from invariant mass measurement alone. The in-medium mass shift and broadening of the width of a particle have been related to the real part of the forward scattering amplitude on the constituents of the medium and thus to the corresponding cross sections. These results indicate a small mass shift but a large increase of the width both in intermediate and high energy heavy ion collisions [5,9,10]. The goal of the present paper is to verify these results using slightly different techniques. We will point out the differences as we proceed.

Recently, dilepton measurements at the CERN/SPS energy have received quite some attention [11]. The e^+e^- mass spectra (in S + Au collision at $E/A = 200$ GeV and in Pb + Au collision at $E/A = 160$ GeV preliminary data) seem to indicate a ρ-peak suppression in central collisions. The absence of ρ-peak may be due to a large width of the ρ meson as compared with its free value. Of course, a confirmation of such a conjecture must include a dynamical simulation for the space time evolution of the colliding system. In any case, it is important to quantitatively address this issue independently.

The in-medium effects on the ρ meson have been widely investigated using finite temperature field theory at the one-loop level [3,12,13], but the most important source for the width modification occurs at the two-loop level [6]. The present paper focuses on the ρ meson width modification up to the two-loop level. The pole shift of the ρ, as emerged from many-body calculations is small [5,8–10].

The in-medium properties of the ρ are due to its interaction with the *constituents* of the medium. In the hadronic matter produced in ultrarelativistic heavy ion collisions, pions and nucleons are important constituents, so we take into account both $\rho\,\pi$ and ρ N reactions in our ρ width calculations. Interactions with other hadrons are expected to increase the width above the values found here.

The paper is organized as follows: In section II, we present the general formulæ for the collision rate of in-medium ρ's. We present a calculation of the thermal averaged in-medium width. In section III, we discuss the cross sections for $\rho\,\pi$- and ρN- reactions from which the collision rates are determined. The width modifications due to $\rho\,\pi$- and ρN- reactions are calculated at finite temperature and density in section IV. Section V concludes with a summary.

II. FORMALISM

The principal elementary reactions which tend to thermalize ρ's in hot and dense matter are the channels $\rho_1\,\pi_2 \to \rho_3\,\pi_4$ and/or $\rho_1\,N_2 \to \rho_3\,N_4$. A ρ with arbitrary momentum p_1 (and energy ω) can be captured by the thermal background. The rate for this direct capture [14] is:

$$\Gamma_d(\omega) = \frac{1}{2\omega}\int d\Omega\, n_2(E_2)\,(1 \pm n_3(E_3))\,(1 \pm n_4(E_4))\,\overline{|\mathcal{M}(12 \to 34)|^2}\quad , \tag{2.1}$$

A ρ with momentum p_1 can also be produced from the thermal background by the inverse reaction: $\rho_3\,\pi_4 \to \rho_1\,\pi_2$. This inverse rate (omitted in many similar treatments) is

$$\Gamma_i(\omega) = \frac{1}{2\omega}\int d\Omega\,(1 \pm n_2(E_2))\,n_3(E_3)\,n_4(E_4)\,\overline{|\mathcal{M}(34 \to 12)|^2}\quad , \tag{2.2}$$

where

$$d\Omega = d\overline{p}_2\,d\overline{p}_3\,d\overline{p}_4\,(2\pi)^4\,\delta(p_1 + p_2 - p_3 - p_4)\,, \tag{2.3}$$

and

$$d\overline{p}_i = \frac{d^3p_i}{(2\pi)^3\,2E_i}\,.$$

$n_i(E_i)$ are Bose-Einstein or Fermi-Dirac distribution functions, '$\pm$' corresponds to Bosons and Fermions, respectively.

The total collision rate for bosons is the difference

$$\Gamma^{\rm coll}(\omega) = \Gamma_d(\omega) - \Gamma_i(\omega)\,. \tag{2.4}$$

This expression can be derived from quantum field theory [15]. From finite temperature quantum field theory, the width of any particle, $\Gamma(\omega)$, is given by the imaginary part of its self-energy, $\mathrm{Im}\Pi(\omega)$,

$$\mathrm{Im}\Pi(\omega) = -\omega\Gamma(\omega)\ , \tag{2.5}$$

which provides a link between field theory and statistical mechanics.

The ratio of $\Gamma_d(\omega)$ to $\Gamma_i(\omega)$ is an universal function of ω [16],

$$\frac{\Gamma_d(\omega)}{\Gamma_i(\omega)} = \exp(\omega/T)\ , \tag{2.6}$$

because the single-particle distribution functions satisfy

$$\begin{aligned} \frac{1+n_B(\omega)}{n_B(\omega)} &= \exp(\omega/T) \quad \text{(Boson)} \quad , \\ \frac{1-n_F(\omega)}{n_F(\omega)} &= \exp(\omega/T) \quad \text{(Fermion)} \quad . \end{aligned} \tag{2.7}$$

Thus the total collision rate is given by:

$$\Gamma^{\rm coll} = (1-e^{-\beta\omega})\,\Gamma_d(\omega)\ . \tag{2.8}$$

In the simplest scenario of equilibrated hot and dense matter, we can calculate the thermal average of the collision rate:

$$\overline{\Gamma}^{\rm coll} = \frac{\int \mathrm{d}^3p_1 \Gamma^{\rm coll}\, n_1(\omega)}{\int \mathrm{d}^3p_1\, n_1(\omega)} = \frac{\int \mathrm{d}^3p_1 \Gamma_d\, e^{-\beta\omega}}{\int \mathrm{d}^3p_1\, n_1(\omega)}\,, \tag{2.9}$$

Using (2.1) and (2.9), the thermal rate can be written as

$$\overline{\Gamma}^{\rm coll} = \frac{\mathcal{N}_1\mathcal{N}_2}{\rho_1}\int_{s_0}^{\infty} \mathrm{d}s \frac{T}{2(2\pi)^4\sqrt{s}}\,\lambda(s,m_1^2,m_2^2)\,\tilde{K}(\sqrt{s},m_1,m_2,T,\mu_i)\,\sigma_{12\to34}(s)\,, \tag{2.10}$$

where

$$\rho_1 = \mathcal{N}_1 \int \frac{\mathrm{d}^3p_1}{(2\pi)^3}\, n_1(\omega) \tag{2.11}$$

is the number density of the ρ's we considered, $\sigma_{12\to 34}(s)$ is the cross section of $\rho\,\pi$ (or $\rho\,N$) collisions, and $s_0 = (m_1 + m_2)^2$, $\mathcal{N}_i$ are the spin-isospin degeneracy factors. The function $\tilde{K}$ assumes different forms for different statistics [17]. Below we apply classical Boltzmann statistics, where

$$\tilde{K} = K_1(\sqrt{s}/T)\exp[(\mu_1 + \mu_2)/T]\,, \tag{2.12}$$

with K_1 being the modified Bessel function. $\mu_1\,, \mu_2$ are the chemical potentials of ρ and π (or nucleon) respectively. From (2.10) the collision rate of ρ in the hot and dense matter can be obtained if the cross sections of the $\rho\,\pi$- or ρN- processes are known.

III. $\rho\pi$ AND ρN CROSS SECTIONS

For $\rho\,\pi$ collisions, we use both the scattering amplitude of the elementary processes method and the resonance contribution approximation to calculate the cross sections $\sigma_{\rho\,\pi}$. We consider the scattering amplitudes for the elementary reactions in Fig. 1 which can be obtained by cutting the two-loop diagrams for the ρ meson self-energy as demonstrated in Ref. [18].

To determine the ρ N cross section $\sigma_{\rho\,N}$, a method based on the resonance model is used to get a lower estimate.

A. $\rho\,\pi$ cross section

The standard Breit-Wigner formula for $\rho\,\pi$ cross section is

$$\sigma_{\rho\,\pi} = \frac{\pi}{q^2}\,\sum_R F_s\,F_i\,\frac{B_R\Gamma_R^2}{(\sqrt{s}-m_R)^2+\Gamma_R^2/4}\quad . \tag{3.1}$$

Here 'R' refers to the intermediate resonance, and B_R is the branching ratio of its decay into $\pi\,\rho$. $\sqrt{s}$ is the total center-of-mass energy, q is the three-momentum of the ρ meson in the resonance frame,

$$q = \frac{1}{2\sqrt{s}}\,\lambda^{1/2}(s, m_\pi^2, m_\rho^2)\,, \tag{3.2}$$

with the kinematical triangle function $\lambda(x,y,z) = x^2 - 2x(y+z) + (y-z)^2$. F_s and F_i are spin and isospin degeneracy factors:

$$F_i = \frac{2I_R+1}{(2I_\pi+1)(2I_\rho+1)} \quad , \qquad F_s = \frac{2J_R+1}{(2s_\pi+1)(2s_\rho+1)} \, . \tag{3.3}$$

We take into account the following resonances: $\phi(1020)$, $a_1(1260)$, $a_2(1320)$, $\omega'(1420)$, $\pi(1670)$, with the properties listed in [19].

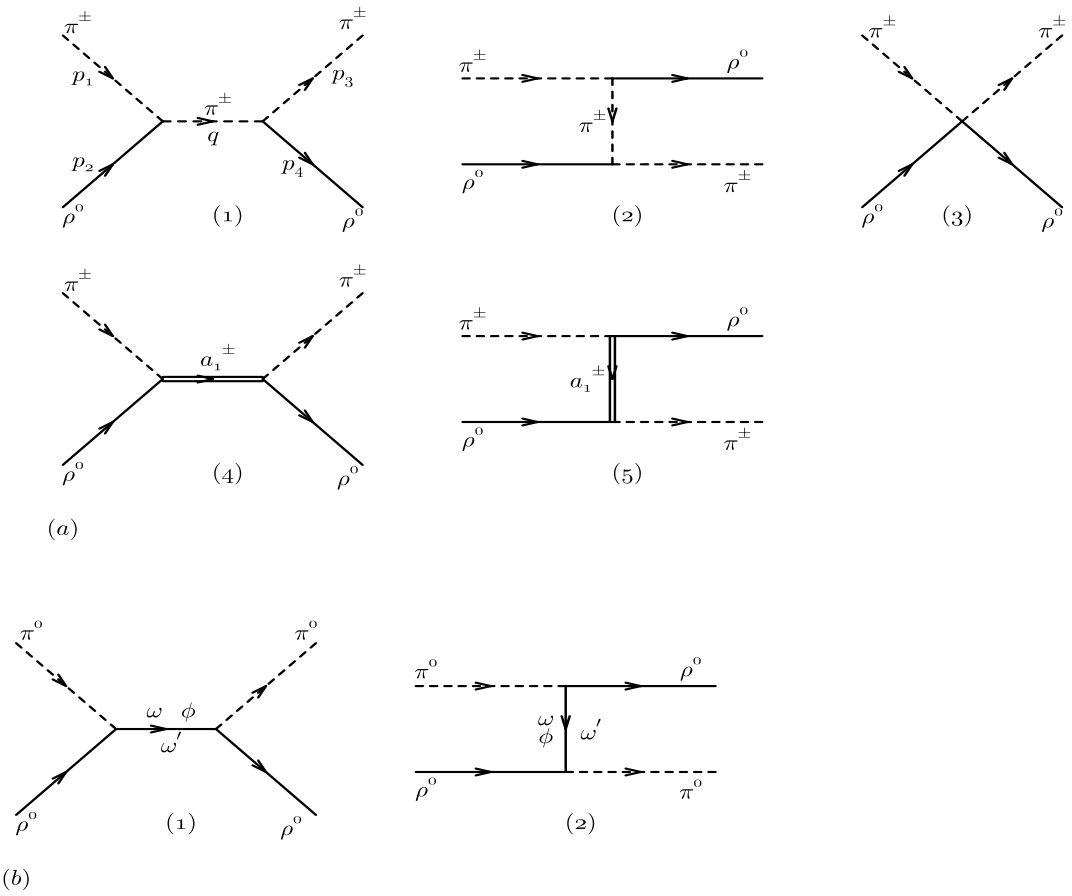

FIG. 1. The Feynman diagrams, (a) for $\rho^0\pi^\pm \to \rho^0\pi^\pm$ reactions and (b) for $\rho^0\pi^0 \to \rho^0\pi^0$ reactions.

The pion scattering amplitude on any hadronic target vanishes at zero pion energy in the target rest frame in the zero pion mass limit (Adler's theorem). Following Ref. [9] one can include an

additional factor to the resonance contributions to $\sigma_{\rho\pi}$,

$$\left(\frac{s-m_\rho^2-m_\pi^2}{m_R^2-m_\rho^2-m_\pi^2}\right)^2 , \tag{3.4}$$

which is normalized to 1 at $s=m_R^2$; for $s>m_R^2$ this factor is taken to be one. The resulting resonant cross section $\sigma_{\rho\pi}$ is shown in Fig. 2(a) (dashed curve).

The cross section for $\rho\pi$ scattering can be calculated by using an effective Lagrangian for the hadronic interaction $\rho\pi\to\rho\pi$. The scattering proceeds through s- and t- channels respectively, where the π, ρ, ω, ϕ, a_1 and $\omega'(1420)$ might be intermediate states. Those processes are constructed from $\pi\pi\rho$, $\pi\rho\omega$ and $\pi\rho a_1$ vertices. The effective interaction Lagrangians we use are the following [20]:

$$\mathcal{L}_{\rho\pi\pi}=ig_{\rho\pi\pi}(\vec{\pi}\times\partial_\mu\vec{\pi})\cdot\vec{\rho}^{\,\mu}\,, \tag{3.5a}$$

$$\mathcal{L}_{\rho\rho\pi\pi}=g_{\rho\pi\pi}^2(\vec{\pi}\times\vec{\rho}_\mu)\cdot(\vec{\pi}\times\vec{\rho}^{\,\mu})\,, \tag{3.5b}$$

$$\mathcal{L}_{\rho\pi\omega}=g_{\rho\pi\omega}\epsilon^{\mu\nu\sigma\tau}\partial_\mu\omega_\nu\partial_\sigma\vec{\rho}_\tau\cdot\vec{\pi}\,. \tag{3.5c}$$

The Lagrangian $\mathcal{L}_{\rho\pi a_1}$ is too long to be presented here [21,22] but for the physical $a_1(k)\to\rho(q)\pi(p)$ decay, for example, the vertex function is

$$\Gamma_{\mu\nu}=i(f_Ag_{\mu\nu}+g_Aq_\mu k_\nu+h_Aq_\mu q_\nu)\,, \tag{3.6}$$

where

$$\begin{aligned} f_A&=\frac{g}{\sqrt{2}}\left[-\eta_1q^2+(\eta_1-\eta_2)k\cdot q\right]\,,\\ g_A&=-\frac{g}{\sqrt{2}}(\eta_1-\eta_2)\,,\\ h_A&=\frac{g}{\sqrt{2}}\eta_1\,. \end{aligned} \tag{3.7}$$

The third term in (3.6) actually does not contribute to the decay width. We chose parameters which reproduce the measured $a_1\to\rho\pi$ decay width and D/S ratio ($g=6.45$, $\eta_1=2.39$ GeV^{-1}, $\eta_2=1.94$ GeV^{-1}). The coupling constant $g_{\rho\pi\pi}=6.05$ is determined from a fit to the free $\rho\to\pi\pi$ decay width, $g_{\rho\pi\omega}=12.40$ GeV^{-1} is determined by the $\omega\to\rho\pi\to\pi\gamma$ decay [20]. The coupling

constant $g_{\rho\pi\omega'} = 3.55$ GeV^{-1} is determined by the $\omega' \to \rho\pi$ decay. Note that we believe that it is important for our effective Lagrangians to generate good phenomenology at energy scales relevant for the applications considered here.

The Feynman diagrams for $\rho\,\pi$ scattering are given in Fig. 1. The cross section is then calculated as

$$\sigma_{\rho\,\pi} = \frac{1}{16\pi\lambda(s, m_\pi^2, m_\rho^2)} \int_{t_-}^{t_+} \mathrm{d}t \overline{|\mathcal{M}|^2}\,, \tag{3.8}$$

where

$$t_\pm = m_\pi^2 + m_\rho^2 - \frac{1}{2s}[(s + m_\pi^2 - m_\rho^2)\,(s - m_\pi^2 + m_\rho^2)] \pm \frac{1}{2s}\lambda(s, m_\pi^2, m_\rho^2)\,. \tag{3.9}$$

For $\rho^0\,\pi^\pm \to \rho^0\,\pi^\pm$ scattering, the squared amplitude is obtained from the processes shown in Fig. 1(a) with the appropriate interference contribution:

$$\overline{|\mathcal{M}|}^2 = \frac{1}{(2s_\pi + 1)(2s_\rho + 1)}\,|\mathcal{M}_1 + \mathcal{M}_2 + \mathcal{M}_3 + \mathcal{M}_4 + \mathcal{M}_5|^2\,, \tag{3.10}$$

which is sum over the spins of the initial states as well as over those of the final states. The $\rho^0\,\pi^\pm \to \rho^\pm\,\pi^0$ scattering is also considered, The squared amplitude has the same form as (3.10) but no contributions from $\mathcal{M}_2$ and $\mathcal{M}_5$. For $\rho^0\,\pi^0$ scattering, Fig. 1(b), $\overline{|\mathcal{M}|}^2$ can be calculated similarly.

Due to the substructure of hadrons, for vertices in the t-channel Feynman diagrams we use form factors

$$F_\alpha = \frac{\Lambda^2 - m_\alpha^2}{\Lambda^2 - t}\,, \tag{3.11}$$

where α indicates the species of the exchange particle. $\Lambda = 1.8$ GeV is taken for all vertices. The numerical integration for the reaction $\rho\,\pi \to \pi \to \rho\,\pi$ (t-channel) results in a singularity. We regulate it with the effective approach of Peierls [23]. This technique offers a pragmatic solution to the possible unitarity violation at high energies that can result from the use of tree-level diagrams. A more complete solution would perhaps comprise a K-matrix multichannel calculation. However, such an endeavor at finite temperature and finite density also carries ambiguities of its own.

After computing the amplitude, the $\pi\,\rho$ scattering cross section is obtained from (3.8). The result is shown in Fig. 2(a) (solid curve). The resulting $\rho\pi$ cross sections indicate that the difference between the resonance model and the scattering amplitude method becomes large at high energies. The resonance model may be valid only at low energies. Our effective Lagrangian technique also treats below-threshold re[illegible]o receives a contribution fro[illegible]ams and all their associated quantum interferences.

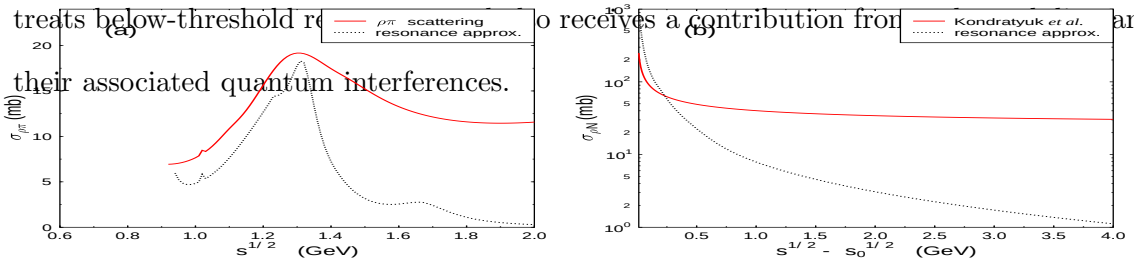

FIG. 2. The cross sections, (a) for $\rho\pi \to \rho\pi$ reactions, and (b) for ρ N $\to \rho$ N reactions.

B. ρ N cross section

The ρ N cross section can be calculated within the resonance model as [9,10],

$$\sigma_{\rho N} = \frac{\pi}{6q^2} \sum_R (2J_R + 1) \frac{B_R \Gamma_R^2}{(\sqrt{s} - M_R)^2 + \Gamma_R^2/4} \quad . \tag{3.12}$$

Here

$$q = \frac{1}{2\sqrt{s}} \lambda^{1/2}(s, m_N^2, m_\rho^2)\,, \tag{3.13}$$

and $\sqrt{s}_0 = m_\rho + m_N$. The summation is performed over all baryonic resonances with masses above the ρN threshold and below 2200 MeV as quoted in [19]. The result of the ρ N cross section calculated from (3.12) is shown in Fig. 2(b) (dashed curve).

The ρ N cross section obtained within the resonance model may be valid only for low energies, while at high energies one should calculate it from the quark model. Furthermore, it has been shown recently that the resonances below the ρ N threshold, like the N*(1520) play an important role in the ρ-nucleon dynamics [24], so in the baryonic sector we adopt the ρ N cross section as determined by Kondratyuk *et al.* Ref [25], which includes also resonances below the ρN threshold. The numerical result is shown in Fig. 2(b) (solid curve).

IV. BROADENING THE WIDTH OF THE RHO AT FINITE TEMPERATURES AND DENSITIES

The modified properties of hadrons in hadronic matter, *e.g.* the width increase of the particles, are due to their interactions with the constituents of the medium. We assume that ultrarelativistic heavy ion collisions generate a hot and dense hadron gas of pions and nucleons and consider the ρ mesons interacting with this thermal gas. We realize that this is a simplification of the complex dynamics which will be generated in all collision of heavy ions. Our results should be taken as lower estimates of the realistic effects.

As discussed in section II, the rho meson width is related to the imaginary part of the rho self-energy. The total width of the ρ meson is the physical decay width plus the collision width,

$$\Gamma_\rho^{\rm total} = \Gamma_\rho^{\rm decay} + \overline{\Gamma}_\rho^{\ \rm coll.} \ . \tag{4.1}$$

The decay width is related to the imaginary part of the rho self-energy at the one-loop level. The collision width is related to the imaginary part of the rho self-energy at the two-loop level. Let us first calculate the decay width of the ρ mesons at finite temperature.

A. The decay width of the rho at finite temperature

To evaluate the ρ meson self-energy from the $\pi\pi$ loop we consider the $\rho\pi\pi$ interaction Lagrangian from the previous section. Using the Feynman rules of thermal field dynamics, the temperature dependent rho meson self-energy is [12]

$$\Pi_{\mu\nu}(q,T) = \frac{g_{\rho\pi\pi}^2}{(2\pi)^3}\int {\rm d}^4k \left\{ -2g_{\mu\nu}\delta(k^2-m_\pi^2)n_\pi(k) + (q+2k)_\mu(q+2k)_\nu \cdot \right. \\ \left. \left[\frac{\delta(k^2-m_\pi^2)}{(k+q)^2-m_\pi^2} n_\pi(k) + \frac{\delta((k+q)^2-m_\pi^2)}{k^2-m_\pi^2} n_\pi(k+q) \right] \right\} \ . \tag{4.2}$$

Because of the lack of Lorentz invariance in the medium [3,12,26], the ρ self-energy at finite temperature separates into a transverse part, $\Pi_T(q,T)$, and a longitudinal part, $\Pi_L(q,T)$. In the rho meson rest frame,

$$\Pi(\omega, \vec{q}\to 0, T) = \Pi_L(\omega, \vec{q}\to 0, T) = \Pi_T(\omega, \vec{q}\to 0, T) \tag{4.3}$$

thus the real part of the self-energy is,

$$\mathrm{Re}\Pi(\omega,\vec{q}\to 0,T) = -\frac{g^2_{\rho\pi\pi}}{3\pi^2}\int \mathrm{d}k\frac{k^2}{E_k}\left(3-\frac{4k^2}{4E_k^2-\omega^2}\right) n_\pi(E_k)\ , \tag{4.4}$$

where $E_k=\sqrt{k^2+m_\pi^2}$. The real self-energy will lead to a mass shift of the ρ at finite temperature, which is determined by the solution of

$$\omega^2 - m_\rho^2 + \mathrm{Re}\Pi(\omega,\vec{q}\to 0,T) = 0\,. \tag{4.5}$$

It is known from previous calculations that this mass shift is small [3].

The imaginary part of the self-energy can be obtained by using cutting rules [16],

$$\mathrm{Im}\Pi(\omega,T) = \frac{g^2_{\rho\pi\pi}}{6\pi}\int \mathrm{d}k\frac{k^4}{E_k}\left(2n_\pi(E_k)+1\right)\quad\left[\delta(\omega+2E_k)-\delta(\omega-2E_k)\right]\ . \tag{4.6}$$

From $\mathrm{Im}\Pi(\omega,T)$, the corresponding width of the $\rho\to\pi\pi$ decay follows to be

$$\Gamma_\rho^{\mathrm{decay}}(T) = \frac{g^2_{\rho\pi\pi}}{48\pi\omega^2}\left(\omega^2-4m_\pi^2\right)^{3/2}\left[2n_\pi(\frac{\omega}{2})+1\right]\ . \tag{4.7}$$

This decay width varies with the temperature as shown in Fig. 3. Obviously the decay width increases with temperature as well as with the pion chemical potential. For $T=150$ MeV, when $\mu_\pi=0$, $\Delta\Gamma_\rho=\Gamma_\rho^{\mathrm{decay}}(T)-\Gamma_\rho^{\mathrm{decay}}(0)=25$ MeV, while for $\mu_\pi=135$ MeV, $\Delta\Gamma_\rho=70$ MeV.

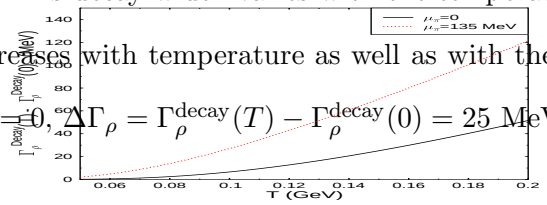

FIG. 3. The $\rho\to\pi\pi$ decay width as a function of temperature T at two fixed values of the pion chemical potential.

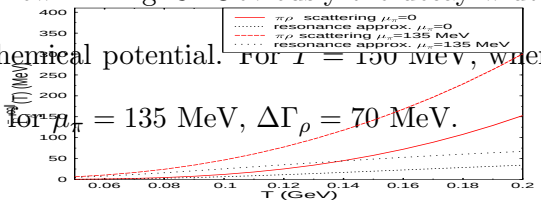

FIG. 4. The ρ collision rate *vs.* the temperature due to $\rho\,\pi$ interaction in two different approaches.

B. Collision rate of rho at finite temperature and density

From (2.10) and with the cross sections computed in the previous section, the collision rates of the ρ mesons can be calculated numerically.

First the rho collision rate is calculated due to $\rho\pi$ reactions in the finite temperature meson medium. The contributions from $\rho^0\pi^\pm\to\rho^0\pi^\pm$, $\rho^0\pi^\pm\to\rho^\pm\pi^0$ and $\rho^0\pi^0\to\rho^0\pi^0$ processes are

taken into account. Fig. 4 shows the the collision rates as calculated from the scattering amplitude calculation and from the Breit-Wigner resonance approximation at two values of the pion chemical potential, $\mu_\pi = 0$ and $\mu_\pi = 135$ MeV. For the same temperature and chemical potentials and using the $\rho\pi$ cross section from the scattering amplitude method, one can get a larger collision rate of ρ mesons.

The collision rate from ρ N reactions is plotted in Fig. 5. In Fig. 5(a), we use $T = 100,\ \ 150$ MeV and show the rate as a function of the nucleon density ratio. In Fig. 5(b), we show the rate as a function of the temperature for two values of the nucleon chemical potential, $\mu_N = 0.4,\ \ 0.6$ GeV. From Fig. 5(a), we can see the collision rate increasing with the nucleon density for a given temperature, but decreasing with temperature for a fixed nucleon density. The latter decrease is due to the fact that the nucleon chemical potential decreases with temperature at a fixed nucleon density. Again we find that for given temperature and chemical potential the pure resonance contribution yields a lower collision rate than the resonance + quark model.

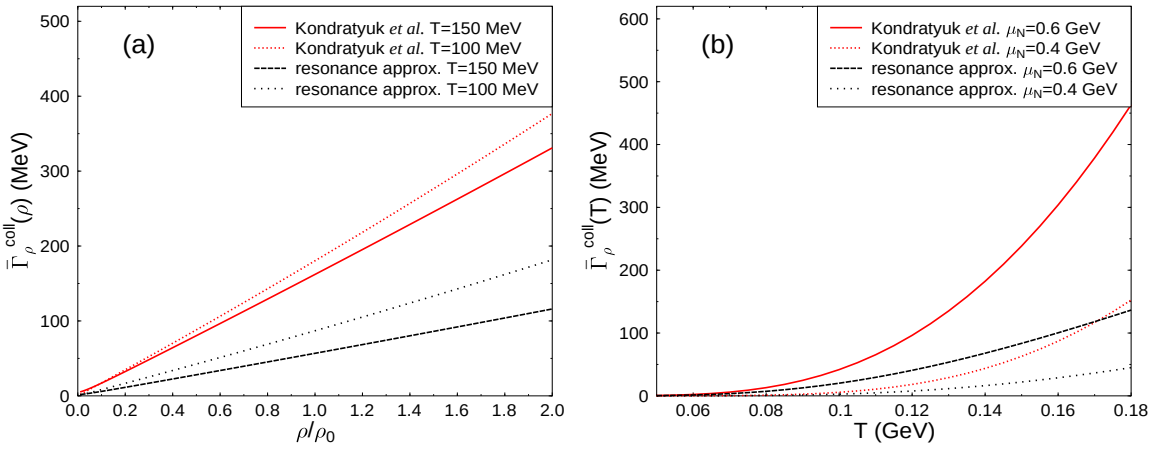

FIG. 5. The collision rate of the ρ due to ρ N interactions, *vs*. (a) the nucleon density for vary temperature. (b) the temperature for vary baryon chemical potential.

We employ the resonance model modified to include the resonances below the ρN threshold, such as N*(1520), as described previously. The total ρN cross section can be evaluated as a function of the invariant collision energy $\sqrt{s}$ and the invariant mass of the ρ meson M_ρ. In this case, the

collision width has to be integrated over the spectral function of the ρ meson as

$$\overline{\Gamma}_{\rho \mathrm{N}} = \frac{\mathcal{N}_1 \mathcal{N}_2}{\rho_1} \int_{s_0'}^{\infty} \mathrm{d}s \frac{T}{2(2\pi)^4 \sqrt{s}} \int_{2m_\pi}^{\sqrt{s}-m_N} \mathrm{d}M_\rho \, M_\rho A(M_\rho) \, \lambda(s, M_\rho^2, m_N^2) \, \tilde{K} \, \sigma_{\rho \mathrm{N}}(s, M_\rho) \,, \tag{4.8}$$

here $s_0' = (2m_\pi + m_N)^2$. $A(M_\rho)$ is the spectral function of the ρ meson in free space taken as

$$A(M_\rho) = \frac{1}{\pi} \frac{m_\rho \Gamma_\rho(M_\rho)}{(M_\rho^2 - m_\rho^2)^2 + m_\rho^2 \Gamma_\rho^2} \,, \tag{4.9}$$

where $m_\rho = 770$ MeV, $\Gamma_\rho(M_\rho)$ is the mass-dependent width of the ρ meson [25]. For the same process of ρN scattering, the collision width of the ρ meson in this calculation is about 10% larger than that from the on mass-shell ρ meson calculations.

In summary, our results indicate that at high temperature and low nucleon density, the collision rate is dominated by ρ + meson reactions, while at low temperature and high nucleon density it is dominated by ρ + nucleon reactions. For example, when $T = 100$ MeV, $\mu_\pi = 0$, $\rho_N = \rho_0$, $\overline{\Gamma}_{\rho\pi}{}^{\mathrm{coll.}} = 12$ MeV, while $\overline{\Gamma}_{\rho N}{}^{\mathrm{coll.}} = 180$MeV.

For conditions typical of high energy heavy-ion collisions [5,27], $T = 150$ MeV, $\mu_\pi = 0$ and $\mu_N = 0.4$ GeV, ($\rho_N = 0.39\rho_0$) the total width of rho mesons is

$$\begin{aligned} \Gamma^{\mathrm{total}} &= \Gamma^{\mathrm{decay}} + \overline{\Gamma}_{\rho\pi}{}^{\mathrm{coll.}} + \overline{\Gamma}_{\rho N}{}^{\mathrm{coll.}} \\ &\approx 176 + 58 + 63 = 297\,\mathrm{MeV} \quad . \end{aligned}$$

This dramatic increase of the ρ width is most certainly important.

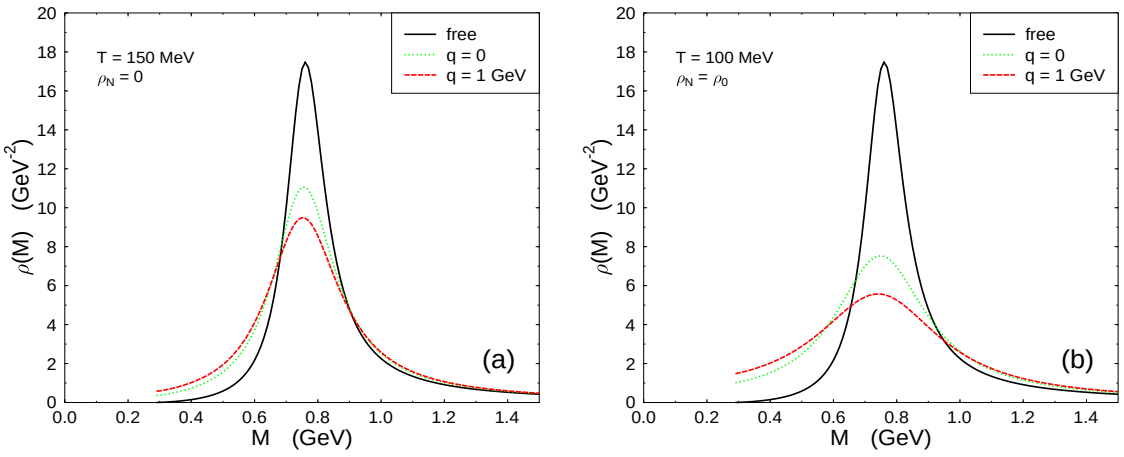

FIG. 6. The spectral function of the ρ *vs.* the invariant mass M of the ρ for fixed values of momentum as indicated. (a) In pure pion gas. (b) In the matter of pions and nucleons.

The spectral function of rho meson is given by

$$\rho(M) = -\frac{2\mathrm{Im}\Pi}{(\omega^2 - q^2 - m_\rho^2 - \mathrm{Re}\Pi)^2 + (\mathrm{Im}\Pi)^2}\,, \tag{4.10}$$

where q is the three-momentum of the ρ meson. The vacuum part of the self-energy Π, which is given in [28], can only depend on the invariant mass $M = \sqrt{\omega^2 - q^2}$. We plot the ρ meson spectral function in fig. 6(a) for a pure pion gas at a temperature $T = 150$ MeV and in fig. 6(b) for the matter of pions and nucleons at $T = 100$ MeV and nucleon density $\rho_N = \rho_0 = 0.16$ fm^{-3}. We find a broadening of the ρ spectral function and a sizable suppression of the peak strength. Because the cross sections from the collision rate are evaluated on the ρ meson mass shell, the imaginary self energy of ρ which comes from the collisions does not vary with M. Therefore the spectral function doesn't vanish when the two-pion threshold is reached.

V. SUMMARY

Based on the idea that in thermal systems a particle can be captured and can also be produced by the thermal background, and the fact that the collision rate is the difference of the capture and the production rate, we have calculated the ρ decay width at finite temperature and the collision rates of the ρ due to the $\rho\,\pi$ scattering and ρN scattering in hot and dense hadronic matter. In high temperature and/or high density hadronic matter, the collision rate is much larger than the decay width correction due to the one-loop self-energy modifications. For the collision rates, the contribution from $\rho\,\pi$ collisions is the most important one in the high temperature pion gas, while at low temperatures and high density nuclear matter the ρN contribution is more important.

The collision rate of ρ mesons with pions uses an effective Lagrangian for the $a_1\rho\pi$ interaction which is tuned to hadronic phenomenology [21,22]. Note that in $\rho\pi \to \rho\pi$ scatterings, the a_1 intermediate state gives the largest contribution to the cross section and to the collision rate. Our result for ρN scattering is in qualitative agreement with the width increase found in [28].

We have shown that the width of the ρ is increased drastically through its interaction with pions and nucleons present in typical heavy-ion collisions. It will be even more increased if finite pion chemical potentials are introduced or if other scattering partners are considered. This result will be important not only for the dilepton spectra, but also for the general dynamics of heavy ion collisions. We believe that our results adds to the consensus building in this direction.

ACKNOWLEDGMENTS

S. Gao thanks the Alexander von Humboldt-Stiftung for financial support. C. G. is happy to acknowledge useful discussions with R. Rapp. This work was supported by the Graduiertenkolleg Theoretische und Experimentelle Schwerionenphysik, BMBF, DFG, GSI, by the Natural Sciences and Engineering Research Council of Canada, and by the Fonds FCAR of the Quebec Government.

---

[1] G. E. Brown and M. Rho, Phys. Rev. Lett. **66**, 2720 (1991).

[2] T. Hatsuda and S. H. Lee, Phys. Rev. **C46**, R34 (1992); R. Furnstahl, T. Hatsuda and S. H. Lee, Phys. Rev. **D42**, 1744 (1890); T. Hatsuda, Y. Koike and S. H. Lee, Nucl. Phys. **B394**, 221, (1993); Phys. Rev. **D47**, 1225 (1993).

[3] C. Gale and J. I. Kapusta, Nucl. Phys. **B357**, 65 (1991).

[4] G. Q. Li, C. M. Ko and G. E. Brown, Phys. Rev. Lett. **75**, 4007 (1995); Nucl. Phys. **A606**, 568 (1996).

[5] G. Chanfray, R. Rapp and J. Wambach, Phys. Rev. Lett. **76**, 368 (1996); R. Rapp, G. Chanfray and J. Wambach, Nucl. Phys. **A617**, 472 (1997).

[6] K. Haglin, Nucl. Phys. **A584**, 719 (1995).

[7] K. Haglin, Phys. Rev. **C53**, R2606 (1996); Phys. Rev. **C54**, 1492 (1996); J. Murray, W. Bauer and K. Haglin, Phys. Rev. **C57**, 1449 (1998).

[8] F. Klingl, N. Kaiser and W. Weise, Nucl. Phys. **A642**, 527 (1997).

[9] V. L. Eletsky and B. L. Ioffe, Phys. Rev. Lett. **78**, 1010 (1997); V. L. Eletsky, B. L. Ioffe and J. I. Kapusta, Eur. J. Phys. **A3**, 381 (1998).

[10] A. Sibirtsev and W. Cassing, Nucl. Phys. **A 629**, 717 (1998).

[11] G. Agakichiev *et al.* CERES Collaboration, Phys. Rev. Lett. **75**, 1272 (1995); P. Wurm, CERES Collaboration, Nucl. Phys. **A590**, 103c (1995); G. Agakichiev *et al.* CERES Collaboration, Nucl. Phys. **A610**, 317c (1996), Phys. Lett. **B402**, 405 (1998).

[12] S. Gao, Y. J. Zhang and R. K. Su, J. Phys. **G21**, 1665 (1995).

[13] H. Shiomo and T. Hatsuda, Phys. Lett. **B334**, 281 (1994); C. Song P. W. Xia and C. M. Ko, Phys. Rev. **C52**, 408 (1995); Y. J. Zhang, S. Gao and R. K. Su, Phys. Rev. **C56**, 3336 (1997); S. Sarkar, J. Alam, P. Roy and B. Sinha, Nucl. Phys. **A634**, 206 (1998).

[14] H. A. Weldon, Z. Phys. **C54**, 431 (1992).

[15] S. Jeon and P. J. Ellis, Phys. Rev. D **58**, 045013 (1998).

[16] H. A. Weldon, Phys. Rev. **D28**, 2007 (1983).

[17] P. Lichard, Phys. Rev. **D49**, 5812 (1994).

[18] J. I. Kapusta, P. Lichard and D. Seibert, Phys. Rev. **D44**, 2774 (1991).

[19] P. Caso *et al.*, Particle Data Group, Eur. Jour. Phys. **C3**, 1 (1998).

[20] G. Janssen, K. Holinde and J. Speth, Phys. Rev. **C 49**, 2763 (1994).

[21] H. Gomm, Ö. Kaymakcalan and J. Schechter, Phys. Rev. **D30**, 2345 (1984).

[22] S. Gao and C. Gale, Phys. Rev. **C57**, 254 (1998).

[23] R. F. Peierls, Phys. Rev. Lett. **6**, 641 (1961).

[24] B. Friman, M. Lutz and G. Wolf, nucl-th/9811040; G. E. Brown, G. Q. Li, R. Rapp, M. Rho

and J. Wambach, Acta Phys.Polon. **B29**, 2309 (1998).

[25] L. A. Kondratyuk, A. Sibirtsev, W. Cassing, Ye. S. Golubeva and M. Effenberger, Phys. Rev. **C58**, 1078 (1998).

[26] J. I. Kapusta, *Finite Temperature Field Theory*, Cambridge University Press, Cambridge 1989.

[27] H. Sorge, Phys. Lett. **B373**, 16 (1996).

[28] V. L. Eletsky, and J. I. Kapusta, nucl-th/9810052.

Rho Meson Broadening in Hot and Dense Hadronic Matter

Song Gao[1], Charles Gale[2], Christoph Ernst[1],

Horst Stöcker[1] and Walter Greiner[1]

[1] *Institut für Theoretische Physik der J.W. Goethe-Universität*

Postfach 111932, D-60054 Frankfurt a. M., Germany

[2] *Physics Department, McGill University*

3600 University St., Montréal, QC, H3A 2T8, Canada

Abstract

The modification of the width of rho mesons due to in-medium decays and collisions is evaluated. The decay width is calculated from the imaginary part of the one-loop self-energy at finite temperature. The collision width is related to the cross sections of the ρ + pion and the ρ + nucleon reactions. A calculation based on an effective Lagrangian shows the importance of including the direct $\rho\pi \to \rho\pi$ scattering which is dominated by the a_1 exchange. A large broadening of the spectral function is found, accompanied by a strength suppression at the pole.

PACS : 25.75.Dw, 14.40Cs, 21.65.+f, 13.75.Lb

I. INTRODUCTION

It is generally believed that ultrarelativistic heavy ion collisions produce matter far from the ground state and provide conditions of high temperature and/or high density suitable for investigating modified particle properties in the medium. The vector mesons, e.g. the rho, are particularly important components of the matter produced in ultrarelativistic heavy ion collisions. It has been speculated that the restoration of chiral symmetry induces a mass shift of the ρ meson [1]. The direct dilepton decay channel, $\rho \to e^+e^-$, appears to be an ideal probe for studying the in-medium properties of the ρ: a possible mass shift, a modified dispersion relation, or a width modification [2–8]. Unfortunately, due to the interplay between those effects, it seems to be difficult to isolate the different effects from invariant mass measurement alone. The in-medium mass shift and broadening of the width of a particle have been related to the real part of the forward scattering amplitude on the constituents of the medium and thus to the corresponding cross sections. These results indicate a small mass shift but a large increase of the width both in intermediate and high energy heavy ion collisions [5,9,10]. The goal of the present paper is to verify these results using slightly different techniques. We will point out the differences as we proceed.

Recently, dilepton measurements at the CERN/SPS energy have received quite some attention [11]. The e^+e^- mass spectra (in S + Au collision at $E/A = 200$ GeV and in Pb + Au collision at $E/A = 160$ GeV preliminary data) seem to indicate a ρ-peak suppression in central collisions. The absence of ρ-peak may be due to a large width of the ρ meson as compared with its free value. Of course, a confirmation of such a conjecture must include a dynamical simulation for the space time evolution of the colliding system. In any case, it is important to quantitatively address this issue independently.

The in-medium effects on the ρ meson have been widely investigated using finite temperature field theory at the one-loop level [3,12,13], but the most important source for the width modification occurs at the two-loop level [6]. The present paper focuses on the ρ meson width modification up to the two-loop level. The pole shift of the ρ, as emerged from many-body calculations is small [5,8–10].

The in-medium properties of the ρ are due to its interaction with the *constituents* of the medium. In the hadronic matter produced in ultrarelativistic heavy ion collisions, pions and nucleons are important constituents, so we take into account both $\rho\,\pi$ and ρ N reactions in our ρ width calculations. Interactions with other hadrons are expected to increase the width above the values found here.

The paper is organized as follows: In section II, we present the general formulæ for the collision rate of in-medium ρ's. We present a calculation of the thermal averaged in-medium width. In section III, we discuss the cross sections for $\rho\,\pi$- and ρN- reactions from which the collision rates are determined. The width modifications due to $\rho\,\pi$- and ρN- reactions are calculated at finite temperature and density in section IV. Section V concludes with a summary.

II. FORMALISM

The principal elementary reactions which tend to thermalize ρ's in hot and dense matter are the channels $\rho_1\,\pi_2 \to \rho_3\,\pi_4$ and/or $\rho_1\,N_2 \to \rho_3\,N_4$. A ρ with arbitrary momentum p_1 (and energy ω) can be captured by the thermal background. The rate for this direct capture [14] is:

$$\Gamma_d(\omega) = \frac{1}{2\omega}\int d\Omega\, n_2(E_2)\,(1 \pm n_3(E_3))\,(1 \pm n_4(E_4))\,\overline{|\mathcal{M}(12 \to 34)|^2}\quad , \tag{2.1}$$

A ρ with momentum p_1 can also be produced from the thermal background by the inverse reaction: $\rho_3\,\pi_4 \to \rho_1\,\pi_2$. This inverse rate (omitted in many similar treatments) is

$$\Gamma_i(\omega) = \frac{1}{2\omega}\int d\Omega\,(1 \pm n_2(E_2))\,n_3(E_3)\,n_4(E_4)\,\overline{|\mathcal{M}(34 \to 12)|^2}\quad , \tag{2.2}$$

where

$$d\Omega = d\overline{p}_2\,d\overline{p}_3\,d\overline{p}_4\,(2\pi)^4\,\delta(p_1 + p_2 - p_3 - p_4)\,, \tag{2.3}$$

and

$$d\overline{p}_i = \frac{d^3p_i}{(2\pi)^3\,2E_i}\,.$$

$n_i(E_i)$ are Bose-Einstein or Fermi-Dirac distribution functions, '$\pm$' corresponds to Bosons and Fermions, respectively.

The total collision rate for bosons is the difference

$$\Gamma^{\rm coll}(\omega) = \Gamma_d(\omega) - \Gamma_i(\omega)\,. \tag{2.4}$$

This expression can be derived from quantum field theory [15]. From finite temperature quantum field theory, the width of any particle, $\Gamma(\omega)$, is given by the imaginary part of its self-energy, ${\rm Im}\Pi(\omega)$,

$${\rm Im}\Pi(\omega) = -\omega\Gamma(\omega)\ , \tag{2.5}$$

which provides a link between field theory and statistical mechanics.

The ratio of $\Gamma_d(\omega)$ to $\Gamma_i(\omega)$ is an universal function of ω [16],

$$\frac{\Gamma_d(\omega)}{\Gamma_i(\omega)} = \exp(\omega/T)\ , \tag{2.6}$$

because the single-particle distribution functions satisfy

$$\begin{aligned} \frac{1+n_B(\omega)}{n_B(\omega)} &= \exp(\omega/T) \quad \text{(Boson)} \quad , \\ \frac{1-n_F(\omega)}{n_F(\omega)} &= \exp(\omega/T) \quad \text{(Fermion)} \quad . \end{aligned} \tag{2.7}$$

Thus the total collision rate is given by:

$$\Gamma^{\rm coll} = (1-e^{-\beta\omega})\,\Gamma_d(\omega)\ . \tag{2.8}$$

In the simplest scenario of equilibrated hot and dense matter, we can calculate the thermal average of the collision rate:

$$\overline{\Gamma}^{\rm coll} = \frac{\int {\rm d}^3p_1 \Gamma^{\rm coll}\, n_1(\omega)}{\int {\rm d}^3p_1\, n_1(\omega)} = \frac{\int {\rm d}^3p_1 \Gamma_d\, e^{-\beta\omega}}{\int {\rm d}^3p_1\, n_1(\omega)}\,, \tag{2.9}$$

Using (2.1) and (2.9), the thermal rate can be written as

$$\overline{\Gamma}^{\rm coll} = \frac{\mathcal{N}_1\mathcal{N}_2}{\rho_1}\int_{s_0}^{\infty} {\rm d}s \frac{T}{2(2\pi)^4\sqrt{s}}\,\lambda(s,m_1^2,m_2^2)\,\tilde{K}(\sqrt{s},m_1,m_2,T,\mu_i)\,\sigma_{12\to 34}(s)\,, \tag{2.10}$$

where

$$\rho_1 = \mathcal{N}_1\int \frac{{\rm d}^3p_1}{(2\pi)^3}\,n_1(\omega) \tag{2.11}$$

is the number density of the ρ's we considered, $\sigma_{12\to 34}(s)$ is the cross section of $\rho\,\pi$ (or ρN) collisions, and $s_0 = (m_1 + m_2)^2$, $\mathcal{N}_i$ are the spin-isospin degeneracy factors. The function $\tilde{K}$ assumes different forms for different statistics [17]. Below we apply classical Boltzmann statistics, where

$$\tilde{K} = K_1(\sqrt{s}/T)\exp[(\mu_1 + \mu_2)/T]\,, \tag{2.12}$$

with K_1 being the modified Bessel function. $\mu_1\,, \mu_2$ are the chemical potentials of ρ and π (or nucleon) respectively. From (2.10) the collision rate of ρ in the hot and dense matter can be obtained if the cross sections of the $\rho\,\pi$- or ρN- processes are known.

III. $\rho\pi$ AND ρN CROSS SECTIONS

For $\rho\,\pi$ collisions, we use both the scattering amplitude of the elementary processes method and the resonance contribution approximation to calculate the cross sections $\sigma_{\rho\,\pi}$. We consider the scattering amplitudes for the elementary reactions in Fig. 1 which can be obtained by cutting the two-loop diagrams for the ρ meson self-energy as demonstrated in Ref. [18].

To determine the ρ N cross section $\sigma_{\rho\,N}$, a method based on the resonance model is used to get a lower estimate.

A. $\rho\,\pi$ cross section

The standard Breit-Wigner formula for $\rho\,\pi$ cross section is

$$\sigma_{\rho\,\pi} = \frac{\pi}{q^2}\,\sum_R F_s\,F_i\,\frac{B_R\Gamma_R^2}{(\sqrt{s}-m_R)^2+\Gamma_R^2/4}\quad . \tag{3.1}$$

Here 'R' refers to the intermediate resonance, and B_R is the branching ratio of its decay into $\pi\,\rho$. $\sqrt{s}$ is the total center-of-mass energy, q is the three-momentum of the ρ meson in the resonance frame,

$$q = \frac{1}{2\sqrt{s}}\,\lambda^{1/2}(s, m_\pi^2, m_\rho^2)\,, \tag{3.2}$$

with the kinematical triangle function $\lambda(x,y,z) = x^2 - 2x(y+z) + (y-z)^2$. F_s and F_i are spin and isospin degeneracy factors:

$$F_i = \frac{2I_R+1}{(2I_\pi+1)(2I_\rho+1)} \quad , \qquad F_s = \frac{2J_R+1}{(2s_\pi+1)(2s_\rho+1)} \, . \tag{3.3}$$

We take into account the following resonances: $\phi(1020)$, $a_1(1260)$, $a_2(1320)$, $\omega'(1420)$, $\pi(1670)$, with the properties listed in [19].

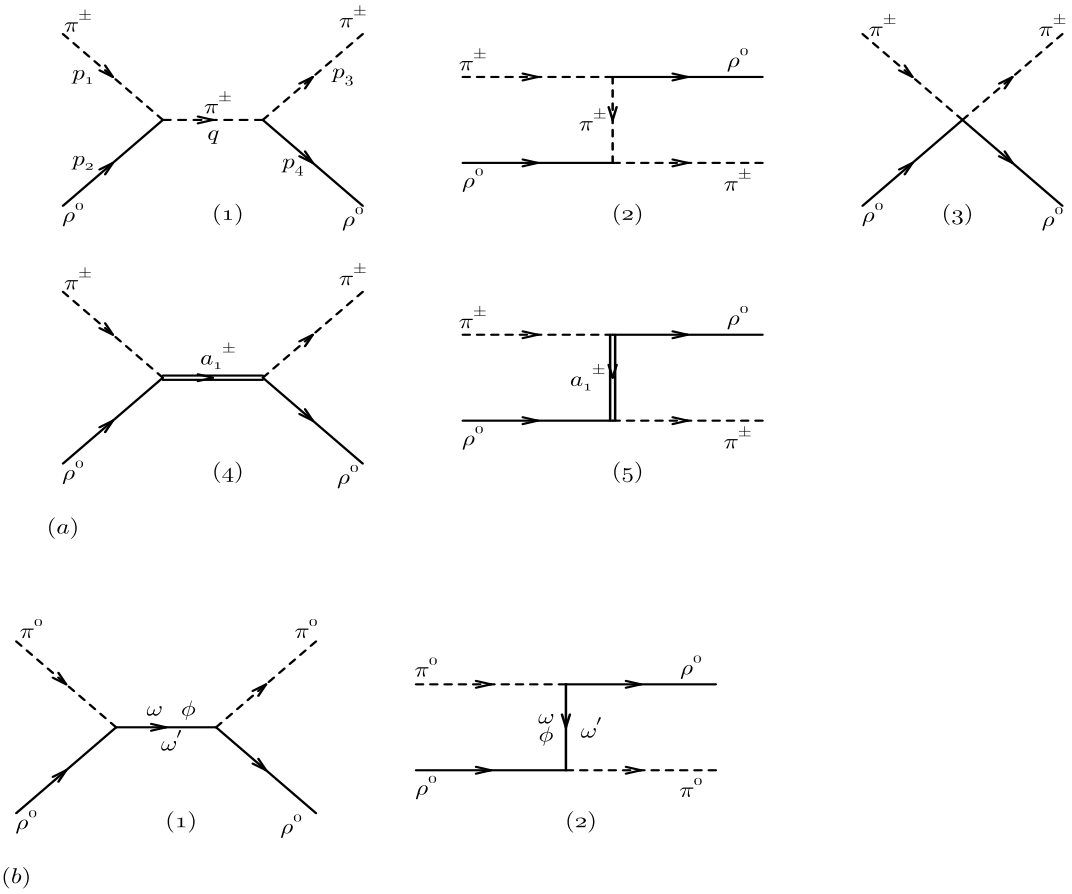

FIG. 1. The Feynman diagrams, (a) for $\rho^0\pi^\pm \to \rho^0\pi^\pm$ reactions and (b) for $\rho^0\pi^0 \to \rho^0\pi^0$ reactions.

The pion scattering amplitude on any hadronic target vanishes at zero pion energy in the target rest frame in the zero pion mass limit (Adler's theorem). Following Ref. [9] one can include an additional factor to the resonance contributions to $\sigma_{\rho\,\pi}$,

$$\left(\frac{s-m_\rho^2-m_\pi^2}{m_R^2-m_\rho^2-m_\pi^2}\right)^2 , \tag{3.4}$$

which is normalized to 1 at $s = m_R^2$; for $s > m_R^2$ this factor is taken to be one. The resulting resonant cross section $\sigma_{\rho\pi}$ is shown in Fig. 2(a) (dashed curve).

The cross section for $\rho\pi$ scattering can be calculated by using an effective Lagrangian for the hadronic interaction $\rho\pi \to \rho\pi$. The scattering proceeds through s- and t- channels respectively, where the π, ρ, ω, ϕ, a_1 and $\omega'(1420)$ might be intermediate states. Those processes are constructed from $\pi\pi\rho$, $\pi\rho\omega$ and $\pi\rho a_1$ vertices. The effective interaction Lagrangians we use are the following [20]:

$$\mathcal{L}_{\rho\pi\pi} = ig_{\rho\pi\pi}(\vec{\pi}\times\partial_\mu\vec{\pi})\cdot\vec{\rho}^{\,\mu}\,, \tag{3.5a}$$

$$\mathcal{L}_{\rho\rho\pi\pi} = g_{\rho\pi\pi}^2(\vec{\pi}\times\vec{\rho}_\mu)\cdot(\vec{\pi}\times\vec{\rho}^{\,\mu})\,, \tag{3.5b}$$

$$\mathcal{L}_{\rho\pi\omega} = g_{\rho\pi\omega}\epsilon^{\mu\nu\sigma\tau}\partial_\mu\omega_\nu\partial_\sigma\vec{\rho}_\tau\cdot\vec{\pi}\,. \tag{3.5c}$$

The Lagrangian $\mathcal{L}_{\rho\pi a_1}$ is too long to be presented here [21,22] but for the physical $a_1(k) \to \rho(q)\pi(p)$ decay, for example, the vertex function is

$$\Gamma_{\mu\nu} = i(f_A g_{\mu\nu} + g_A q_\mu k_\nu + h_A q_\mu q_\nu)\,, \tag{3.6}$$

where

$$\begin{aligned} f_A &= \frac{g}{\sqrt{2}}\left[-\eta_1 q^2 + (\eta_1-\eta_2)k\cdot q\right]\,, \\ g_A &= -\frac{g}{\sqrt{2}}(\eta_1-\eta_2)\,, \\ h_A &= \frac{g}{\sqrt{2}}\eta_1\,. \end{aligned} \tag{3.7}$$

The third term in (3.6) actually does not contribute to the decay width. We chose parameters which reproduce the measured $a_1 \to \rho\pi$ decay width and D/S ratio ($g = 6.45$, $\eta_1 = 2.39$ GeV^{-1}, $\eta_2 = 1.94$ GeV^{-1}). The coupling constant $g_{\rho\pi\pi} = 6.05$ is determined from a fit to the free $\rho \to \pi\pi$ decay width, $g_{\rho\pi\omega} = 12.40$ GeV^{-1} is determined by the $\omega \to \rho\pi \to \pi\gamma$ decay [20]. The coupling

constant $g_{\rho\pi\omega'} = 3.55$ GeV^{-1} is determined by the $\omega' \to \rho\pi$ decay. Note that we believe that it is important for our effective Lagrangians to generate good phenomenology at energy scales relevant for the applications considered here.

The Feynman diagrams for $\rho\,\pi$ scattering are given in Fig. 1. The cross section is then calculated as

$$\sigma_{\rho\,\pi} = \frac{1}{16\pi\lambda(s, m_\pi^2, m_\rho^2)} \int_{t_-}^{t_+} \mathrm{d}t \overline{|\mathcal{M}|^2}\,, \tag{3.8}$$

where

$$t_\pm = m_\pi^2 + m_\rho^2 - \frac{1}{2s}[(s + m_\pi^2 - m_\rho^2)\,(s - m_\pi^2 + m_\rho^2)] \pm \frac{1}{2s}\lambda(s, m_\pi^2, m_\rho^2)\,. \tag{3.9}$$

For $\rho^0\,\pi^\pm \to \rho^0\,\pi^\pm$ scattering, the squared amplitude is obtained from the processes shown in Fig. 1(a) with the appropriate interference contribution:

$$\overline{|\mathcal{M}|}^2 = \frac{1}{(2s_\pi + 1)(2s_\rho + 1)} \left|\mathcal{M}_1 + \mathcal{M}_2 + \mathcal{M}_3 + \mathcal{M}_4 + \mathcal{M}_5\right|^2, \tag{3.10}$$

which is sum over the spins of the initial states as well as over those of the final states. The $\rho^0\,\pi^\pm \to \rho^\pm\,\pi^0$ scattering is also considered, The squared amplitude has the same form as (3.10) but no contributions from $\mathcal{M}_2$ and $\mathcal{M}_5$. For $\rho^0\,\pi^0$ scattering, Fig. 1(b), $\overline{|\mathcal{M}|}^2$ can be calculated similarly.

Due to the substructure of hadrons, for vertices in the t-channel Feynman diagrams we use form factors

$$F_\alpha = \frac{\Lambda^2 - m_\alpha^2}{\Lambda^2 - t}\,, \tag{3.11}$$

where α indicates the species of the exchange particle. $\Lambda = 1.8$ GeV is taken for all vertices. The numerical integration for the reaction $\rho\,\pi \to \pi \to \rho\,\pi$ (t-channel) results in a singularity. We regulate it with the effective approach of Peierls [23]. This technique offers a pragmatic solution to the possible unitarity violation at high energies that can result from the use of tree-level diagrams. A more complete solution would perhaps comprise a K-matrix multichannel calculation. However, such an endeavor at finite temperature and finite density also carries ambiguities of its own.

After computing the amplitude, the $\pi\,\rho$ scattering cross section is obtained from (3.8). The result is shown in Fig. 2(a) (solid curve). The resulting $\rho\pi$ cross sections indicate that the difference between the resonance model and the scattering amplitude method becomes large at high energies. The resonance model may be valid only at low energies. Our effective Lagrangian technique also treats below-threshold resonances and also receives a contribution from t-channel diagrams and all their associated quantum interferences.

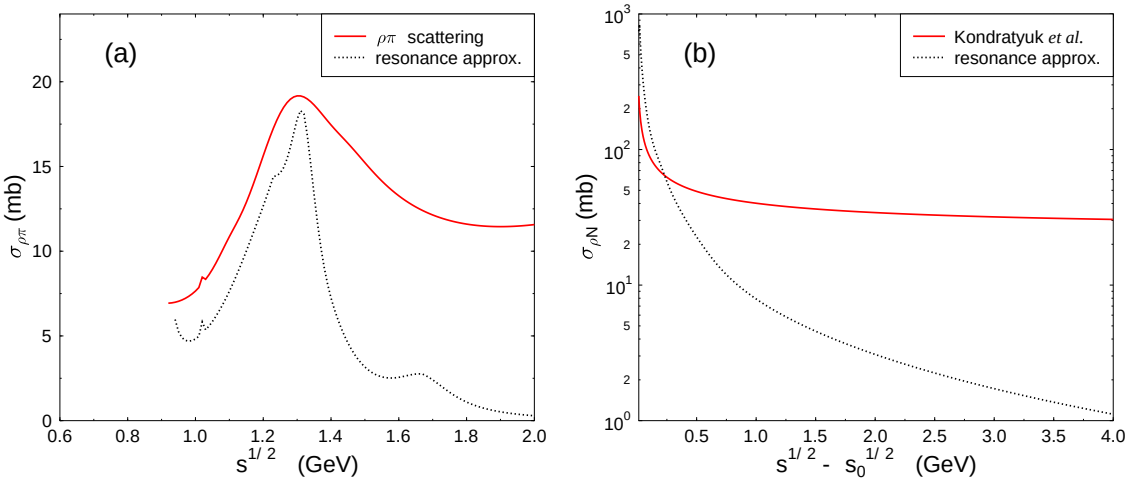

FIG. 2. The cross sections, (a) for $\rho\pi \to \rho\pi$ reactions, and (b) for ρ N $\to \rho$ N reactions.

B. ρN cross section

The ρN cross section can be calculated within the resonance model as [9,10],

$$\sigma_{\rho N} = \frac{\pi}{6q^2} \sum_R (2J_R + 1) \frac{B_R \Gamma_R^2}{(\sqrt{s} - M_R)^2 + \Gamma_R^2/4} \quad . \tag{3.12}$$

Here

$$q = \frac{1}{2\sqrt{s}} \lambda^{1/2}(s, m_N^2, m_\rho^2)\,, \tag{3.13}$$

and $\sqrt{s_0} = m_\rho + m_N$. The summation is performed over all baryonic resonances with masses above the ρN threshold and below 2200 MeV as quoted in [19]. The result of the ρN cross section calculated from (3.12) is shown in Fig. 2(b) (dashed curve).

The ρN cross section obtained within the resonance model may be valid only for low energies, while at high energies one should calculate it from the quark model. Furthermore, it has been shown recently that the resonances below the ρ N threshold, like the N*(1520) play an important role in the ρ-nucleon dynamics [24], so in the baryonic sector we adopt the ρN cross section as determined by Kondratyuk *et al.* Ref [25], which includes also resonances below the ρN threshold. The numerical result is shown in Fig. 2(b) (solid curve).

IV. BROADENING THE WIDTH OF THE RHO AT FINITE TEMPERATURES AND DENSITIES

The modified properties of hadrons in hadronic matter, *e.g.* the width increase of the particles, are due to their interactions with the constituents of the medium. We assume that ultrarelativistic heavy ion collisions generate a hot and dense hadron gas of pions and nucleons and consider the ρ mesons interacting with this thermal gas. We realize that this is a simplification of the complex dynamics which will be generated in all collision of heavy ions. Our results should be taken as lower estimates of the realistic effects.

As discussed in section II, the rho meson width is related to the imaginary part of the rho self-energy. The total width of the ρ meson is the physical decay width plus the collision width,

$$\Gamma_\rho^{\rm total} = \Gamma_\rho^{\rm decay} + \overline{\Gamma}_\rho^{\rm coll.} . \tag{4.1}$$

The decay width is related to the imaginary part of the rho self-energy at the one-loop level. The collision width is related to the imaginary part of the rho self-energy at the two-loop level. Let us first calculate the decay width of the ρ mesons at finite temperature.

A. The decay width of the rho at finite temperature

To evaluate the ρ meson self-energy from the $\pi\pi$ loop we consider the $\rho\pi\pi$ interaction Lagrangian from the previous section. Using the Feynman rules of thermal field dynamics, the temperature dependent rho meson self-energy is [12]

$$\Pi_{\mu\nu}(q,T) = \frac{g^2_{\rho\pi\pi}}{(2\pi)^3}\int \mathrm{d}^4k \left\{ -2g_{\mu\nu}\delta(k^2-m_\pi^2)n_\pi(k) + (q+2k)_\mu(q+2k)_\nu \cdot \right. \\ \left. \left[\frac{\delta(k^2-m_\pi^2)}{(k+q)^2-m_\pi^2} n_\pi(k) + \frac{\delta((k+q)^2-m_\pi^2)}{k^2-m_\pi^2} n_\pi(k+q) \right] \right\} \ . \tag{4.2}$$

Because of the lack of Lorentz invariance in the medium [3,12,26], the ρ self-energy at finite temperature separates into a transverse part, $\Pi_T(q,T)$, and a longitudinal part, $\Pi_L(q,T)$. In the rho meson rest frame,

$$\Pi(\omega,\vec{q}\to 0,T) = \Pi_L(\omega,\vec{q}\to 0,T) = \Pi_T(\omega,\vec{q}\to 0,T) \tag{4.3}$$

thus the real part of the self-energy is,

$$\mathrm{Re}\Pi(\omega,\vec{q}\to 0,T) = -\frac{g^2_{\rho\pi\pi}}{3\pi^2}\int \mathrm{d}k \frac{k^2}{E_k}\left(3 - \frac{4k^2}{4E_k^2-\omega^2}\right) n_\pi(E_k) \ , \tag{4.4}$$

where $E_k = \sqrt{k^2+m_\pi^2}$. The real self-energy will lead to a mass shift of the ρ at finite temperature, which is determined by the solution of

$$\omega^2 - m_\rho^2 + \mathrm{Re}\Pi(\omega,\vec{q}\to 0,T) = 0\,. \tag{4.5}$$

It is known from previous calculations that this mass shift is small [3].

The imaginary part of the self-energy can be obtained by using cutting rules [16],

$$\mathrm{Im}\Pi(\omega,T) = \frac{g^2_{\rho\pi\pi}}{6\pi}\int \mathrm{d}k \frac{k^4}{E_k}\left(2n_\pi(E_k)+1\right) \quad \left[\delta(\omega+2E_k) - \delta(\omega-2E_k)\right] \ . \tag{4.6}$$

From $\mathrm{Im}\Pi(\omega,T)$, the corresponding width of the $\rho\to\pi\pi$ decay follows to be

$$\Gamma_\rho^{\mathrm{decay}}(T) = \frac{g^2_{\rho\pi\pi}}{48\pi\omega^2}\left(\omega^2-4m_\pi^2\right)^{3/2}\left[2n_\pi(\frac{\omega}{2})+1\right] \ . \tag{4.7}$$

This decay width varies with the temperature as shown in Fig. 3. Obviously the decay width increases with temperature as well as with the pion chemical potential. For $T = 150$ MeV, when $\mu_\pi = 0$, $\Delta\Gamma_\rho = \Gamma_\rho^{\mathrm{decay}}(T) - \Gamma_\rho^{\mathrm{decay}}(0) = 25$ MeV, while for $\mu_\pi = 135$ MeV, $\Delta\Gamma_\rho = 70$ MeV.

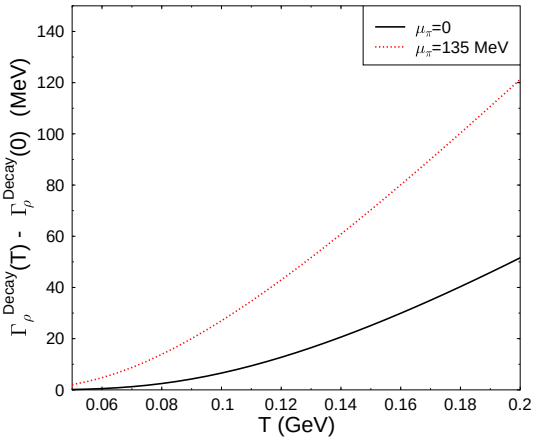

FIG. 3. The $\rho \to \pi\pi$ decay width as a function of temperature T at two fixed values of the pion chemical potential.

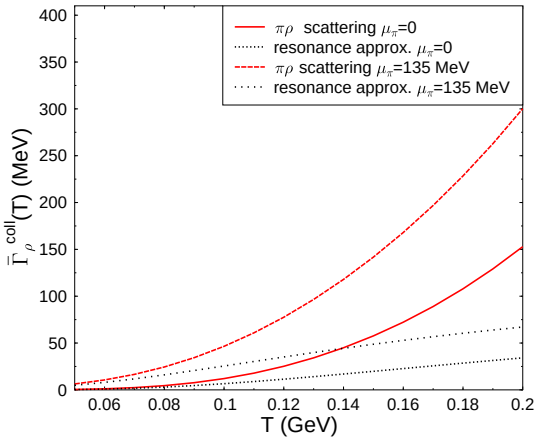

FIG. 4. The ρ collision rate $vs.$ the temperature due to $\rho\,\pi$ interaction in two different approaches.

B. Collision rate of rho at finite temperature and density

From (2.10) and with the cross sections computed in the previous section, the collision rates of the ρ mesons can be calculated numerically.

First the rho collision rate is calculated due to $\rho\pi$ reactions in the finite temperature meson medium. The contributions from $\rho^0\pi^\pm \to \rho^0\pi^\pm$, $\rho^0\pi^\pm \to \rho^\pm\pi^0$ and $\rho^0\pi^0 \to \rho^0\pi^0$ processes are taken into account. Fig. 4 shows the the collision rates as calculated from the scattering amplitude calculation and from the Breit-Wigner resonance approximation at two values of the pion chemical potential, $\mu_\pi = 0$ and $\mu_\pi = 135$ MeV. For the same temperature and chemical potentials and using the $\rho\pi$ cross section from the scattering amplitude method, one can get a larger collision rate of ρ mesons.

The collision rate from ρ N reactions is plotted in Fig. 5. In Fig. 5(a), we use $T = 100,\ \ 150$ MeV and show the rate as a function of the nucleon density ratio. In Fig. 5(b), we show the rate as a function of the temperature for two values of the nucleon chemical potential, $\mu_N = 0.4,\ \ 0.6$ GeV. From Fig. 5(a), we can see the collision rate increasing with the nucleon density for a given

temperature, but decreasing with temperature for a fixed nucleon density. The latter decrease is due to the fact that the nucleon chemical potential decreases with temperature at a fixed nucleon density. Again we find that for given temperature and chemical potential the pure resonance contribution yields a lower collision rate than the resonance + quark model.

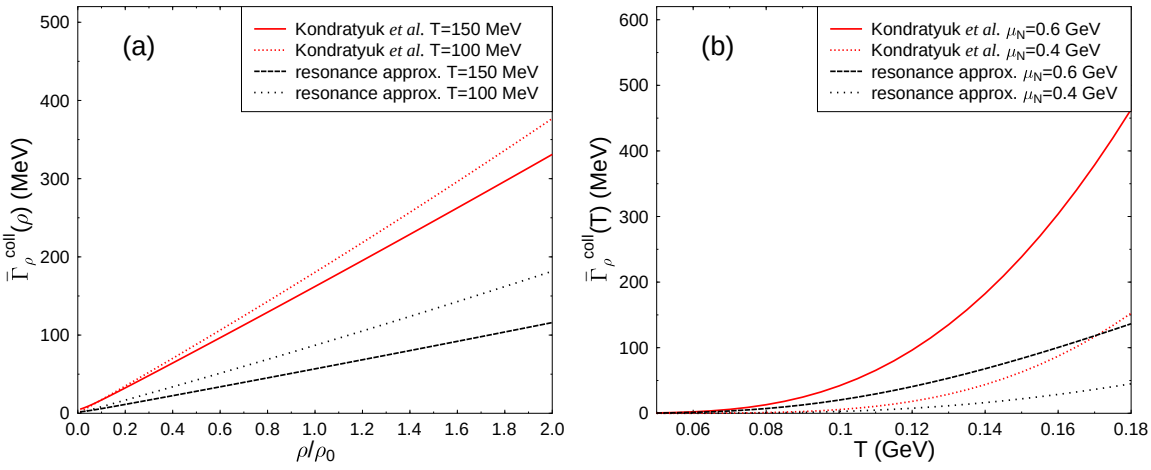

FIG. 5. The collision rate of the ρ due to ρ N interactions, *vs.* (a) the nucleon density for vary temperature. (b) the temperature for vary baryon chemical potential.

We employ the resonance model modified to include the resonances below the ρN threshold, such as N*(1520), as described previously. The total ρN cross section can be evaluated as a function of the invariant collision energy $\sqrt{s}$ and the invariant mass of the ρ meson M_ρ. In this case, the collision width has to be integrated over the spectral function of the ρ meson as

$$\overline{\Gamma}_{\rho\mathrm{N}} = \frac{\mathcal{N}_1\mathcal{N}_2}{\rho_1}\int_{s_0'}^{\infty} \mathrm{d}s \frac{T}{2(2\pi)^4\sqrt{s}} \int_{2m_\pi}^{\sqrt{s}-m_N} \mathrm{d}M_\rho\, M_\rho A(M_\rho)\, \lambda(s, M_\rho^2, m_N^2)\, \tilde{K}\, \sigma_{\rho\mathrm{N}}(s, M_\rho)\,, \tag{4.8}$$

here $s_0' = (2m_\pi + m_N)^2$. $A(M_\rho)$ is the spectral function of the ρ meson in free space taken as

$$A(M_\rho) = \frac{1}{\pi}\frac{m_\rho \Gamma_\rho(M_\rho)}{(M_\rho^2 - m_\rho^2)^2 + m_\rho^2\Gamma_\rho^2}\,, \tag{4.9}$$

where $m_\rho = 770$ MeV, $\Gamma_\rho(M_\rho)$ is the mass-dependent width of the ρ meson [25]. For the same process of ρN scattering, the collision width of the ρ meson in this calculation is about 10% larger than that from the on mass-shell ρ meson calculations.

In summary, our results indicate that at high temperature and low nucleon density, the collision rate is dominated by ρ + meson reactions, while at low temperature and high nucleon density it is dominated by ρ + nucleon reactions. For example, when $T = 100$ MeV, $\mu_\pi = 0$, $\rho_N = \rho_0$, $\overline{\Gamma}_{\rho\pi}^{\rm coll.} = 12$ MeV, while $\overline{\Gamma}_{\rho N}^{\rm coll.} = 180$MeV.

For conditions typical of high energy heavy-ion collisions [5,27], $T = 150$ MeV, $\mu_\pi = 0$ and $\mu_N = 0.4$ GeV, ($\rho_N = 0.39\rho_0$) the total width of rho mesons is

$$\Gamma^{\rm total} = \Gamma^{\rm decay} + \overline{\Gamma}_{\rho\pi}^{\rm coll.} + \overline{\Gamma}_{\rho N}^{\rm coll.}$$
$$\approx 176 + 58 + 63 = 297\,{\rm MeV} \quad .$$

This dramatic increase of the ρ width is most certainly important.

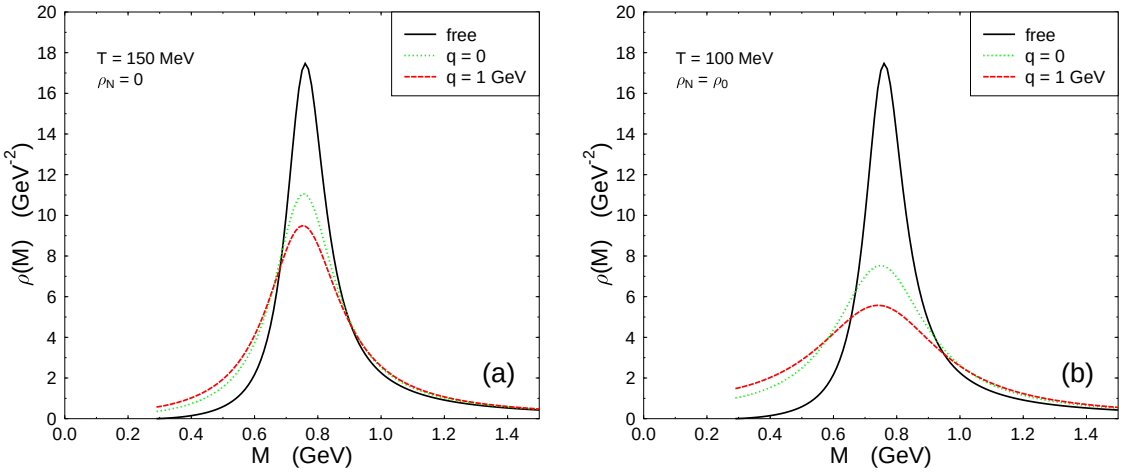

FIG. 6. The spectral function of the ρ *vs.* the invariant mass M of the ρ for fixed values of momentum as indicated. (a) In pure pion gas. (b) In the matter of pions and nucleons.

The spectral function of rho meson is given by

$$\rho(M) = -\frac{2{\rm Im}\Pi}{(\omega^2 - q^2 - m_\rho^2 - {\rm Re}\Pi)^2 + ({\rm Im}\Pi)^2}\,, \tag{4.10}$$

where q is the three-momentum of the ρ meson. The vacuum part of the self-energy Π, which is given in [28], can only depend on the invariant mass $M = \sqrt{\omega^2 - q^2}$. We plot the ρ meson spectral function in fig. 6(a) for a pure pion gas at a temperature $T = 150$ MeV and in fig. 6(b) for the

matter of pions and nucleons at $T = 100$ MeV and nucleon density $\rho_N = \rho_0 = 0.16$ fm^{-3}. We find a broadening of the ρ spectral function and a sizable suppression of the peak strength. Because the cross sections from the collision rate are evaluated on the ρ meson mass shell, the imaginary self energy of ρ which comes from the collisions does not vary with M. Therefore the spectral function doesn't vanish when the two-pion threshold is reached.

V. SUMMARY

Based on the idea that in thermal systems a particle can be captured and can also be produced by the thermal background, and the fact that the collision rate is the difference of the capture and the production rate, we have calculated the ρ decay width at finite temperature and the collision rates of the ρ due to the $\rho\,\pi$ scattering and ρN scattering in hot and dense hadronic matter. In high temperature and/or high density hadronic matter, the collision rate is much larger than the decay width correction due to the one-loop self-energy modifications. For the collision rates, the contribution from $\rho\,\pi$ collisions is the most important one in the high temperature pion gas, while at low temperatures and high density nuclear matter the ρN contribution is more important.

The collision rate of ρ mesons with pions uses an effective Lagrangian for the $a_1\rho\pi$ interaction which is tuned to hadronic phenomenology [21,22]. Note that in $\rho\pi \to \rho\pi$ scatterings, the a_1 intermediate state gives the largest contribution to the cross section and to the collision rate. Our result for ρN scattering is in qualitative agreement with the width increase found in [28].

We have shown that the width of the ρ is increased drastically through its interaction with pions and nucleons present in typical heavy-ion collisions. It will be even more increased if finite pion chemical potentials are introduced or if other scattering partners are considered. This result will be important not only for the dilepton spectra, but also for the general dynamics of heavy ion collisions. We believe that our results adds to the consensus building in this direction.

ACKNOWLEDGMENTS

S. Gao thanks the Alexander von Humboldt-Stiftung for financial support. C. G. is happy to acknowledge useful discussions with R. Rapp. This work was supported by the Graduiertenkolleg Theoretische und Experimentelle Schwerionenphysik, BMBF, DFG, GSI, by the Natural Sciences and Engineering Research Council of Canada, and by the Fonds FCAR of the Quebec Government.

---

[1] G. E. Brown and M. Rho, Phys. Rev. Lett. **66**, 2720 (1991).

[2] T. Hatsuda and S. H. Lee, Phys. Rev. **C46**, R34 (1992); R. Furnstahl, T. Hatsuda and S. H. Lee, Phys. Rev. **D42**, 1744 (1890); T. Hatsuda, Y. Koike and S. H. Lee, Nucl. Phys. **B394**, 221, (1993); Phys. Rev. **D47**, 1225 (1993).

[3] C. Gale and J. I. Kapusta, Nucl. Phys. **B357**, 65 (1991).

[4] G. Q. Li, C. M. Ko and G. E. Brown, Phys. Rev. Lett. **75**, 4007 (1995); Nucl. Phys. **A606**, 568 (1996).

[5] G. Chanfray, R. Rapp and J. Wambach, Phys. Rev. Lett. **76**, 368 (1996); R. Rapp, G. Chanfray and J. Wambach, Nucl. Phys. **A617**, 472 (1997).

[6] K. Haglin, Nucl. Phys. **A584**, 719 (1995).

[7] K. Haglin, Phys. Rev. **C53**, R2606 (1996); Phys. Rev. **C54**, 1492 (1996); J. Murray, W. Bauer and K. Haglin, Phys. Rev. **C57**, 1449 (1998).

[8] F. Klingl, N. Kaiser and W. Weise, Nucl. Phys. **A642**, 527 (1997).

[9] V. L. Eletsky and B. L. Ioffe, Phys. Rev. Lett. **78**, 1010 (1997); V. L. Eletsky, B. L. Ioffe and J. I. Kapusta, Eur. J. Phys. **A3**, 381 (1998).

[10] A. Sibirtsev and W. Cassing, Nucl. Phys. **A 629**, 717 (1998).

[11] G. Agakichiev *et al.* CERES Collaboration, Phys. Rev. Lett. **75**, 1272 (1995); P. Wurm, CERES Collaboration, Nucl. Phys. **A590**, 103c (1995); G. Agakichiev *et al.* CERES Collaboration, Nucl. Phys. **A610**, 317c (1996), Phys. Lett. **B402**, 405 (1998).

[12] S. Gao, Y. J. Zhang and R. K. Su, J. Phys. **G21**, 1665 (1995).

[13] H. Shiomo and T. Hatsuda, Phys. Lett. **B334**, 281 (1994); C. Song P. W. Xia and C. M. Ko, Phys. Rev. **C52**, 408 (1995); Y. J. Zhang, S. Gao and R. K. Su, Phys. Rev. **C56**, 3336 (1997); S. Sarkar, J. Alam, P. Roy and B. Sinha, Nucl. Phys. **A634**, 206 (1998).

[14] H. A. Weldon, Z. Phys. **C54**, 431 (1992).

[15] S. Jeon and P. J. Ellis, Phys. Rev. D **58**, 045013 (1998).

[16] H. A. Weldon, Phys. Rev. **D28**, 2007 (1983).

[17] P. Lichard, Phys. Rev. **D49**, 5812 (1994).

[18] J. I. Kapusta, P. Lichard and D. Seibert, Phys. Rev. **D44**, 2774 (1991).

[19] P. Caso *et al.*, Particle Data Group, Eur. Jour. Phys. **C3**, 1 (1998).

[20] G. Janssen, K. Holinde and J. Speth, Phys. Rev. **C 49**, 2763 (1994).

[21] H. Gomm, Ö. Kaymakcalan and J. Schechter, Phys. Rev. **D30**, 2345 (1984).

[22] S. Gao and C. Gale, Phys. Rev. **C57**, 254 (1998).

[23] R. F. Peierls, Phys. Rev. Lett. **6**, 641 (1961).

[24] B. Friman, M. Lutz and G. Wolf, nucl-th/9811040; G. E. Brown, G. Q. Li, R. Rapp, M. Rho and J. Wambach, Acta Phys.Polon. **B29**, 2309 (1998).

[25] L. A. Kondratyuk, A. Sibirtsev, W. Cassing, Ye. S. Golubeva and M. Effenberger, Phys. Rev. **C58**, 1078 (1998).

[26] J. I. Kapusta, *Finite Temperature Field Theory*, Cambridge University Press, Cambridge 1989.

[27] H. Sorge, Phys. Lett. **B373**, 16 (1996).

[28] V. L. Eletsky, and J. I. Kapusta, nucl-th/9810052.